NLPO analysis of a free standing house with the SLaMA method
Module 3 – Harmonisatie berekeningsmethode

Tavus, A.; Messali, F.

Publication date
2020

Document Version
Final published version

Citation (APA)
Tavus, A., & Messali, F. (2020). *NLPO analysis of a free standing house with the SLaMA method: Module 3 – Harmonisatie berekeningsmethode*. Delft University of Technology.

Project number	CM1B13
File reference	CM1B13-R04
Date	19 October 2020
Corresponding author	Francesco Messali (f.messali@tudelft.nl)

Module 3 – Harmonisatie berekeningsmethode

NLPO ANALYSIS OF A FREE-STANDING HOUSE WITH THE SLAMA METHOD

Authors: Ahmet Tavus, Francesco Messali

***Cite as**: Tavus, A., Messali, F. NLPO analysis of a free-standing house with the SLaMA method - Module 3 – Harmonisatie berekeningsmethode. Report no. CM1B13-R04, Version 01, 19 October 2020. Delft University of Technology*

This document is made available via the website 'Structural Response to Earthquakes' and the TU Delft repository. While citing, please verify if there are recent updates of this research in the form of scientific papers.

This research work was funded by y Stichting Koninklijk Nederlands Normalisatie Instituut (NEN) under project number 8505400024-001.

Table of Contents

1 Introduction

This report summarizes the results of the nonlinear pushover (NLPO) analysis performed with the SLaMA method for a free-standing house in support to the development of NPR 9998 Module 3.

The analysed building is hereinafter referred as "Building A".

For the sake of simplicity, where the following text refers to an article, a section or an Annex "of NPR", this is in fact referring to NPR 9998 [1]. The spectra used for the site specific assessments are taken from the NEN webtool [2].

The NLPO analyses are performed in accordance to the SLaMA method as described in Section G of NPR. The individual capacity of the elements is computed as described in sections G.9.2 for piers and G.9.3 for spandrels. The local acceptance criteria of NPR are considered to assess the performance of the building as described for piers in sections G.9.2.2 and G.9.2.3 for piers, and in section G.9.3.1 for spandrels.

A short description of the SLaMA procedure and of the assumptions made is given in section 2.

Building A is evaluated without considering the soil-structure interaction (SSI) effects, and a fixed based analysis is performed.

2 SLaMA method and assumptions

The SLaMA analyses are performed according to the procedure and the equations recommended in Annex G of NPR.

Each analysis is based on the following steps and assumptions:

- Each perforated wall (i.e. each façade or internal wall) is divided into single elements. The meshing procedure follows the recommendations reported in Section G.9.2.1 of NPR, based on the identification of the compressive struts in the walls (Figure 1a). An example of the mesh of a façade is presented in Figure 1b.
- The roof (i.e. whatever lies above the attic level) is not modelled, but its mass is accounted for.
- Only the inner leaves of the cavity walls are modelled.
- RC floors are able to restrain the rotations at the top of the piers on which they are supported (i.e. the piers are assumed to be double clamped); timber floors are not. In the latter case, the piers are assumed to behave as cantilever elements unless the adjacent spandrels are strong enough to prevent the rotations. This condition occurs when the force acting on the spandrel needed to guarantee the equilibrium with the force acting at failure at the top of the pier (assumed as double clamped) does not exceed the flexural or shear resistance of the spandrel.
- The vertical loads acting on each pier and contributing to the structural stability are computed by considering the initial static configuration. No load is transferred to non-loadbearing walls.
- The possible contribution of the flanges is accounted for according to the method of Moon [3]. The flanges are assumed to be present only between loadbearing walls, for which the interlocking at corners is possible.
- The contribution of the non-loadbearing walls is also included. However, since they have no overburden in the initial stage and they are assumed to be disconnected from the loadbearing walls, their force capacity is based on the self-weight only and it is therefore extremely limited.
- The second order effects are taken into account for each pier as reported in Section 4.4.2.2 of NPR.
- The capacity of each single perforated wall is evaluated separately for every storey. That is computed by summing up the capacity of the individual members at that level.
- The capacity of the structure is then computed for the whole building at each storey level. When the floor is sufficiently stiff to provide a box-behaviour (i.e. if the piers are connected at top by a RC floor which is assumed to be able to redistribute the forces), the contributions of the different perforated walls are summed up. With timber floors, the capacity is computed separately for each perforated wall, and the minimum capacity in terms of normalized accelerations (see the next point) is considered.
- The capacity is scaled by the effective mass of the sub-structure (for two-storey buildings, either the whole building or the top storey only). The capacity of the sub-systems is then presented in terms of accelerations and a comparison is made to identify the sub-structure whose failure is governing (i.e. reaches the lowest acceleration).
- Both modal and mass proportional distribution of the lateral loads are considered. The masses are localised at the floor level.
- For the modal distribution of the lateral loads, an approximated linear distribution is assumed for the sake of simplicity.

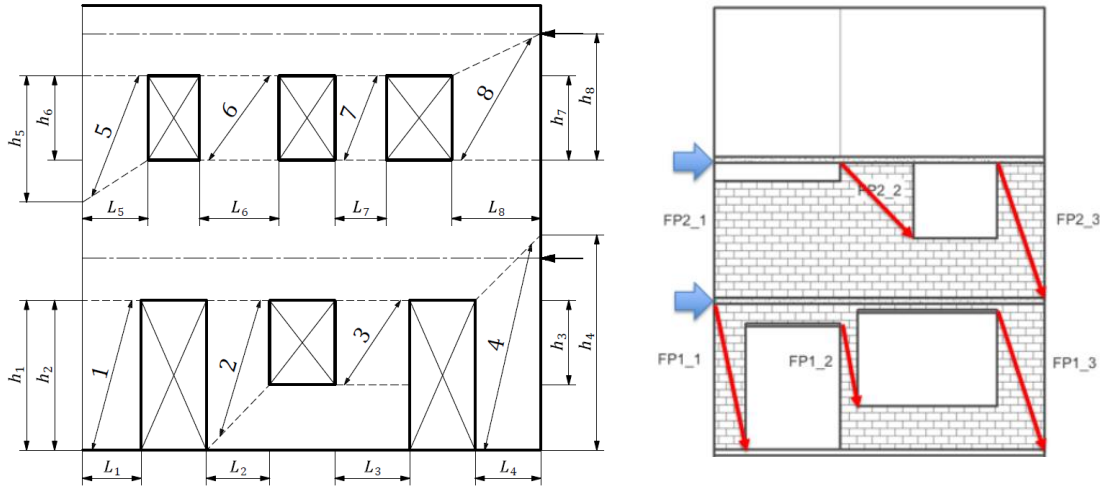

(a) (b)

Figure 1. Graphical representation of the compressive struts of a perforated wall as recommended in [2] (a), and example of meshing of a façade (b).

3 SLaMA calculation of Building A

Building A is a two-storey (plus attic) building, built in 1996. The building is made of unreinforced masonry (URM) cavity walls. Additionally, a one-storey building appendix is part of the structure, but it has not been modelled, since it is structurally connect to the rest of the building only via the roof and the veneers (both elements not included in the SLaMA calculations). A picture and a plane section of the building is shown in Figure 2. The part of the building which is modelled is highlighted; conversely the annex is not (as also indicated by the red cross).

(a) (b)

Figure 2. Building A: picture (a) and plan of the ground floor with orientation (b). In the plan, the part of the building modelled is highlighted.

The discretization of the four facades is shown in Figure 3 to Figure 6 for the positive and negative loading in both the X- and Y- direction. The internal walls are all modelled as cantilever piers, not connected to any other wall, with the exception of wall "RP1_7", which is a load-bearing wall and it is modelled as double clamped wall (as shown in Figure 7). As mentioned in Section 2, the spandrels are not modelled in presence of a RC slab which constrain the rotations at the top of the piers. Specifically, no spandrels are modelled on the East and West wall, with the exception of the annex. The high band of masonry on top of the piers at the ground floor on the North and South façades is also assumed to be able to retain the rotations at the top of the piers for the X-loading direction. For the piers at first storey level on the North and South walls, whose section varies in length throughout the height, the minimum length is considered conservatively.
The effective mass computed for the building is 66.5 t, assuming the first mode shape as linear.

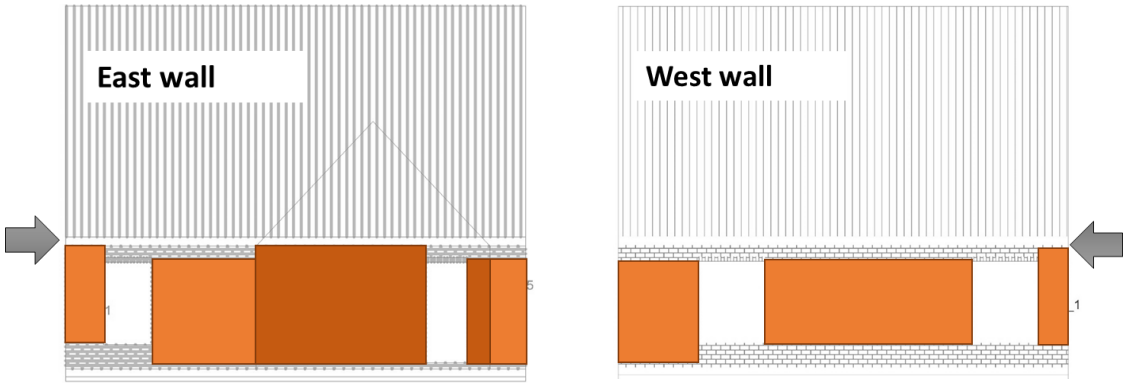

Figure 3. Piers defined on the east and west walls of the Building A for the positive loading (south to north) in the Y-direction. The darker colour indicates the piers on the wall of the annex.

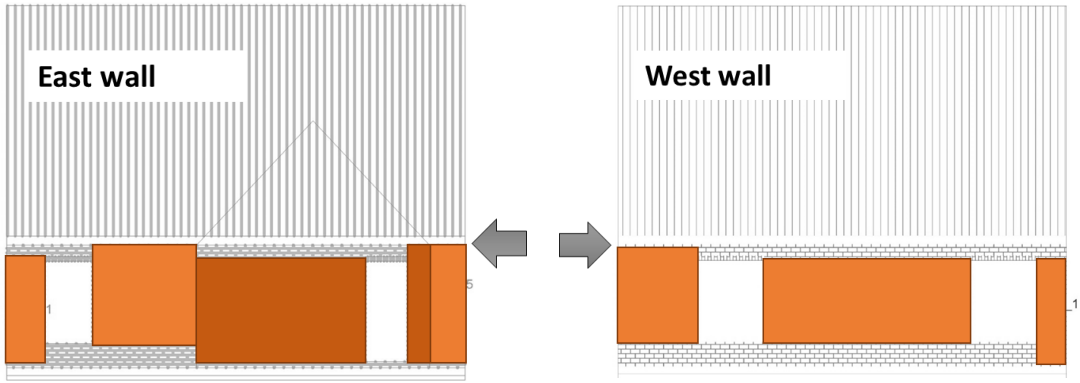

Figure 4. Piers defined on the east and west walls of Building A for the negative loading (north to south) in the Y-direction. The darker colour indicates the piers on the wall of the annex.

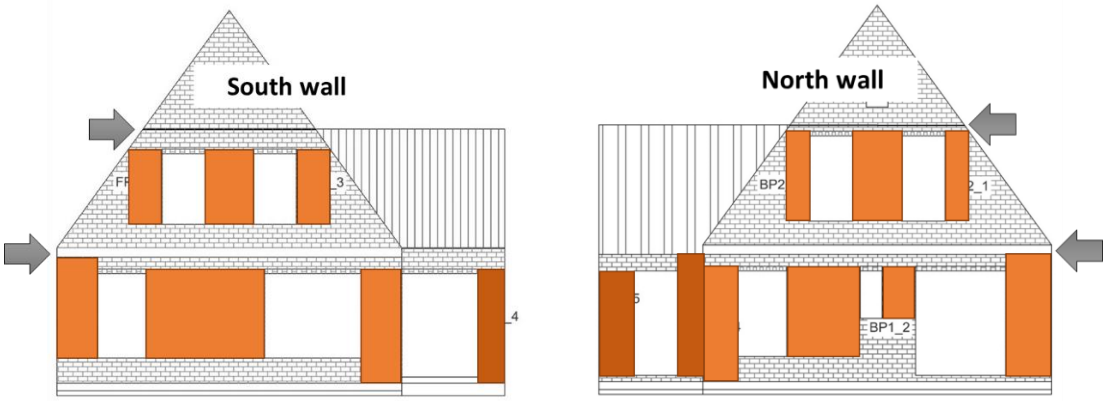

Figure 5. Piers defined on the east and west walls of Building A for the positive loading (west to east) in the X-direction. The darker colour indicates the piers on the wall of the annex.

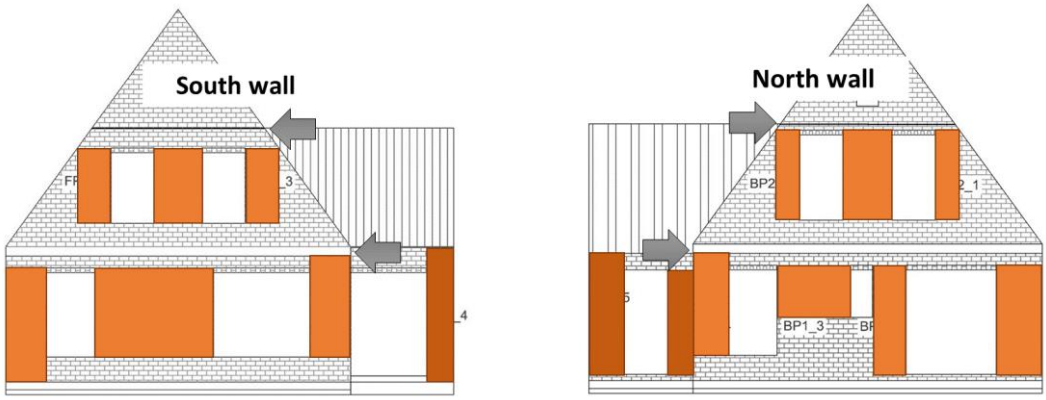

Figure 6. Piers defined on the east and west walls of Building A for the negative loading (east to west) in the X-direction. The darker colour indicates the piers on the wall of the annex.

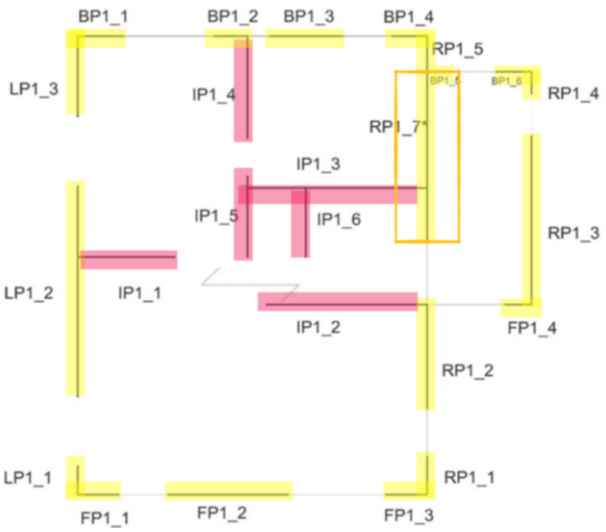

Figure 7. Plan of the ground storey level: identification of loadbearing (yellow) and non-loadbearing (red) walls. The pier RP1_7 is identified by an orange rectangle.

3.1 Positive Y-direction (South-to-North)

Since in the Y-direction all the loadbearing piers are located only at the ground storey level, the capacity curve is computed for that level only. In addition, the capacity of the non-loadbearing inner-piers at the first storey level is computed in order to assess the possible local collapse of such walls. For these walls, the force capacity is normalized with respect to the self-weight of the piers.
The capacity curve obtained for the ground storey level and for the non-loadbearing piers at the first storey are shown in Figure 8. It can be observed that the force capacity of both the piers at top storey is lower than the capacity of the ground storey level (in terms of normalized accelerations). For this reason, a storey mechanism at the ground-storey level is expected to govern the global behaviour of the structure, but the local failure of the piers at the top-storey is possible at an earlier stage.
The mode-proportional distribution of the lateral loads is governing.

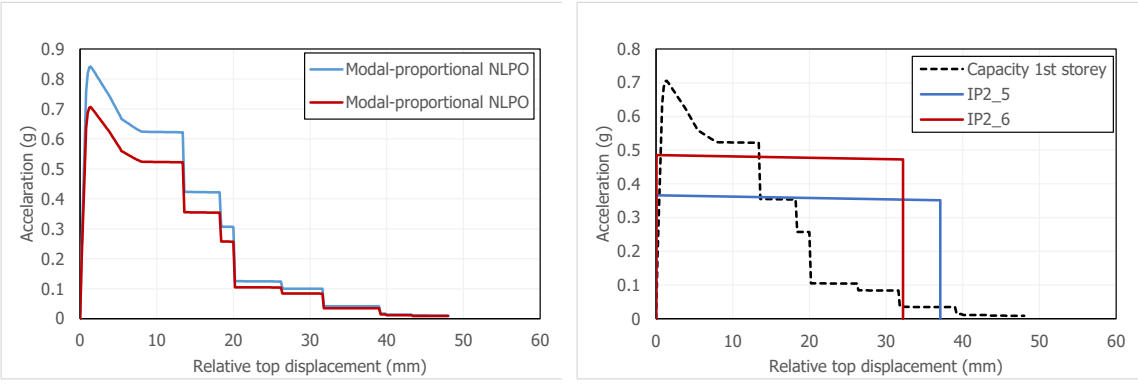

(a) (b)

Figure 8. Capacity curve of the ground (a) and first (b) storey level for the positive loading direction.

The type of failure observed in each pier at ground floor (either shear – as described in section G.9.2.2 of NPR9998 – or flexure – section G.9.2.3) is shown in Figure 9. The blue colour represents flexural failure and

the green colour shear failure. Four long piers (whose which carry the highest base shear) undergo shear failure, so that the capacity curve presents large drops of capacity at relatively small displacements (below 20 mm). Also pier RP1_7, not shown in the figure, undergoes shear failure, whereas all the non-loadbearing piers fail in flexure, including the two piers at the second storey level.

The "brittle" behaviour is shown also by the equivalent bilinear curve derived for the structure and shown in Figure 10 (for the governing mode-proportional lateral load distribution). This curve shows a yielding point at 0.85 mm, for an acceleration of 0.63g, and a NC displacement at 13.6 mm, corresponding to a 0.5% interstorey drift, consistent with the limitations recommended at global level.

The near collapse (NC) displacement is computed at the point corresponding to a 50% drop of the force capacity with respect to the peak load, which corresponds to the collapse of the first long wall. In fact, the difference between the peak and the residual capacity for shear sliding contributes already to a significant drop of capacity, in addition to the collapse of the central pier of the west wall. The sequence of failure of the piers is shown in Figure 11 (it should be noted that the piers with a green number fail before the 50% drop, whereas those with a red number fail after that point).

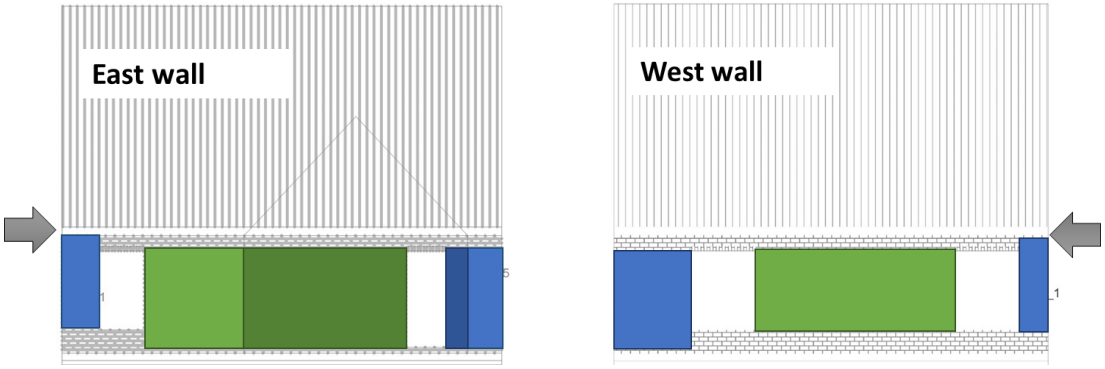

Figure 9. Failure of the piers of the east and west wall for positive loading in the Y-direction. The blue colour represents a flexural failure and the green colour a shear failure.

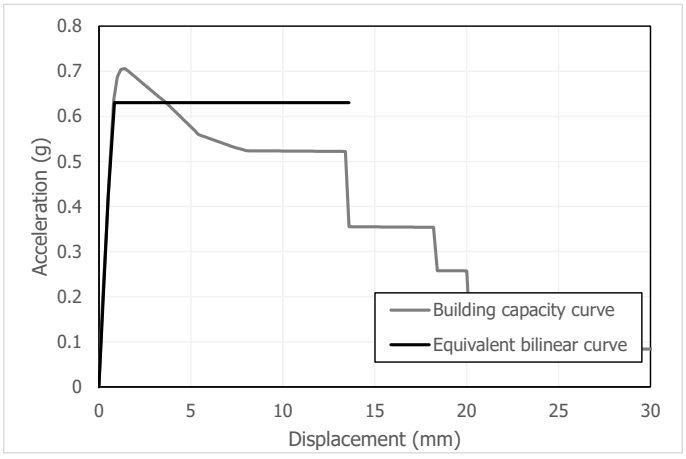

Figure 10. Equivalent bilinear capacity curve derived for the mode-proportional NLPO.

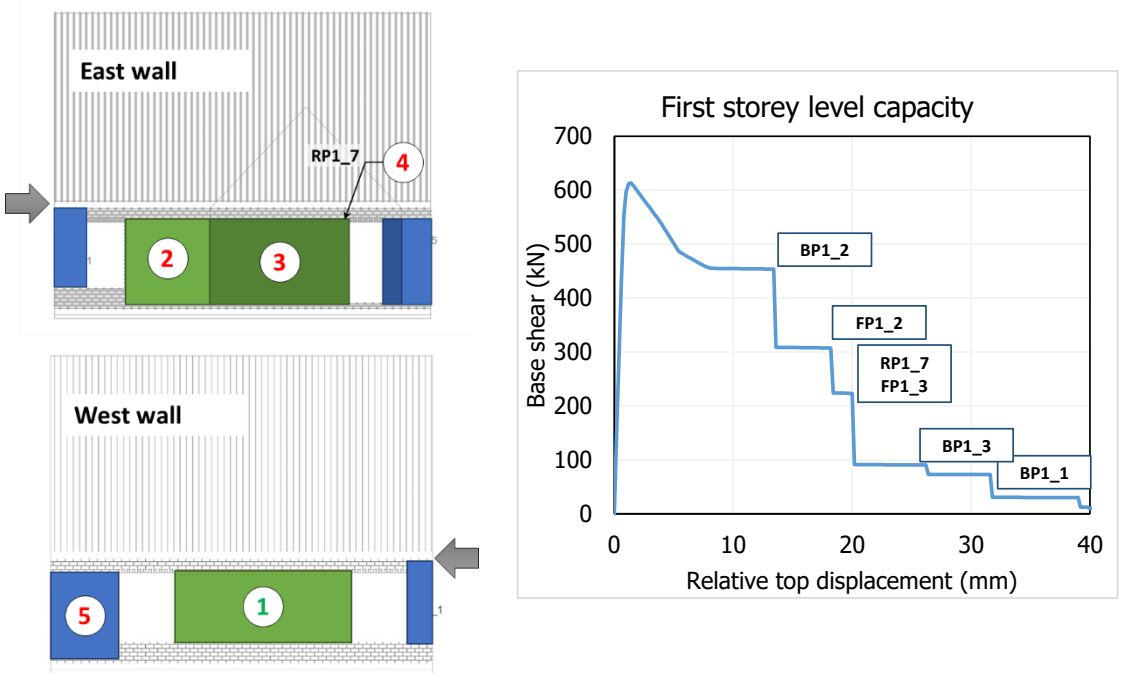

Figure 11. Sequence of NC collapse of the piers on the east and west walls. The piers with a green number fail before the 50% drop, whereas those with a red number fail after that point.

The compliance of the building to NPR9998 is assessed for a specific site by comparing the bilinear capacity curve with the nonlinear ADRS demand. As shown in Figure 12, the building complies to NPR9998 as regards the global in-plane capacity, since the performance point can be find on the capacity curve for a displacement of 0.5 mm, still in the elastic branch of the capacity curve. At this displacement, the system has a ductility factor of 1, so that the elastic ADRS curve is considered.

The spectrum which corresponds to a unity capacity over demand (C/D) ratio is defined by scaling the initial spectrum considered for the site-specific assessment. It should be noted that in principle this is not correct, since each location has several parameters which define the corresponding spectrum and these parameters do not change proportionally. However, the calculation provides a reasonable estimate of the maximum PGA for which the building remains compliant to the NPR9998 recommendations. The scaled spectrum has a PGA of 0.325 g, as shown in Figure 13.

However, it should be recalled that the collapse of two non-loadbearing walls located at the first storey level is expected for lower values of PGA.

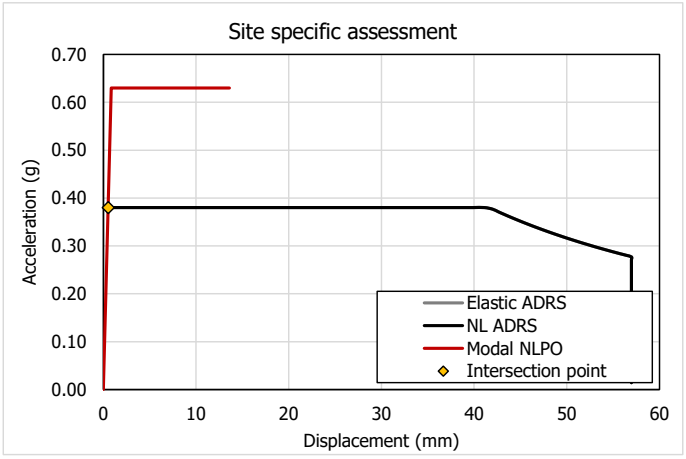

Figure 12. Site specific assessment for mode-proportional NLPO.

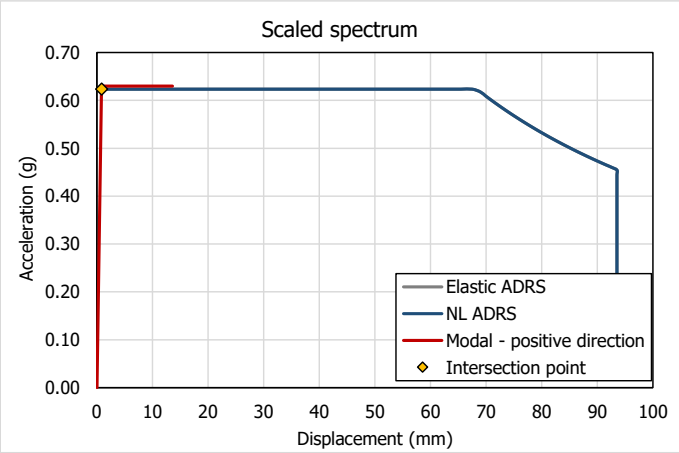

Figure 13. Scaled PGA assessment for mode-proportional NLPO.

3.2 Negative Y-direction (North-to-South)

Similar to the positive direction, the capacity curve is computed for the ground storey level only. In addition, the capacity of the non-loadbearing inner-piers at the first storey level is computed in order to assess the possible local collapse of such walls. Once more, for these walls, the force capacity is normalized with respect to the self-weight of the pier.

The capacity curve obtained for the ground storey level and for the non-loadbearing piers at the first storey are shown in Figure 14. Again, the force capacity of both the piers at top storey is lower than the capacity of the ground storey level (in terms of normalized accelerations). For this reason, a storey mechanism at the ground-storey level is expected to govern the global behaviour of the structure, but the local failure of the piers at the top-storey is possible at an earlier stage.

The mode-proportional distribution of the lateral loads is governing.

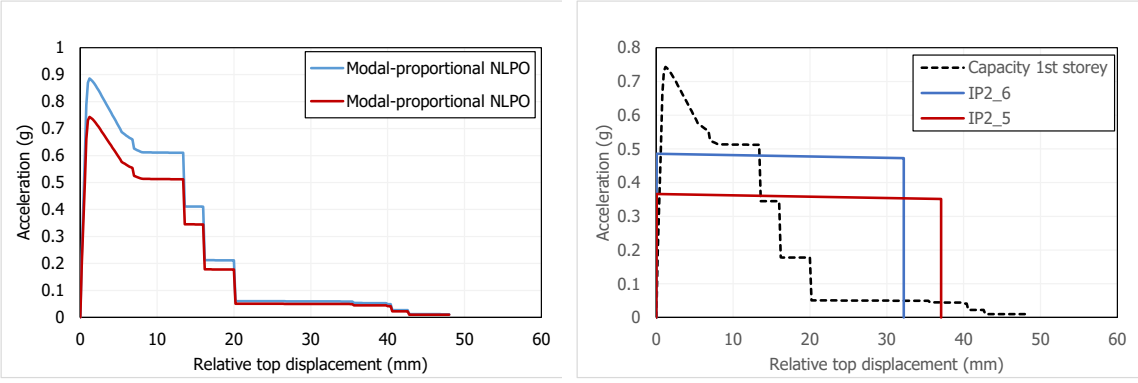

(a) (b)

Figure 14. Capacity curve of the ground (a) and first (b) storey level for the positive loading direction.

The type of failure observed in each pier at ground floor (either shear – as described in section G.9.2.2 of NPR9998 – or flexure – section G.9.2.3) is shown in Figure 15. The blue colour represents flexural failure and the green colour shear failure. Four long piers (whose which carry the highest base shear) undergo shear failure, so that the capacity curve presents large drops of capacity at relatively small displacements (below 20

mm). Also pier RP1_7, not shown in the figure, shows shear failure, whereas all the non-loadbearing piers fail in flexure, including the two piers at the second storey level.
The "brittle" behaviour is shown also by the equivalent bilinear curve derived for the structure and shown in Figure 16 (for the governing mode-proportional lateral load distribution). This curve shows a yielding point at 0.85 mm, for an acceleration of 0.63g, and a NC displacement at 13.6 mm, corresponding to a 0.5% interstorey drift, consistent with the limitations recommended at global level.
The near collapse (NC) displacement is computed at the point corresponding to a 50% drop of the force capacity with respect to the peak load, which corresponds to the collapse of the first long wall. In fact, the difference between the peak and the residual capacity for shear sliding contributes already to a significant drop of capacity, in addition to the collapse of the central pier of the west wall. The sequence of failure of the piers is shown in Figure 17 (it should be noted that the piers with a green number fail before the 50% drop, whereas those with a red number fail after that point).

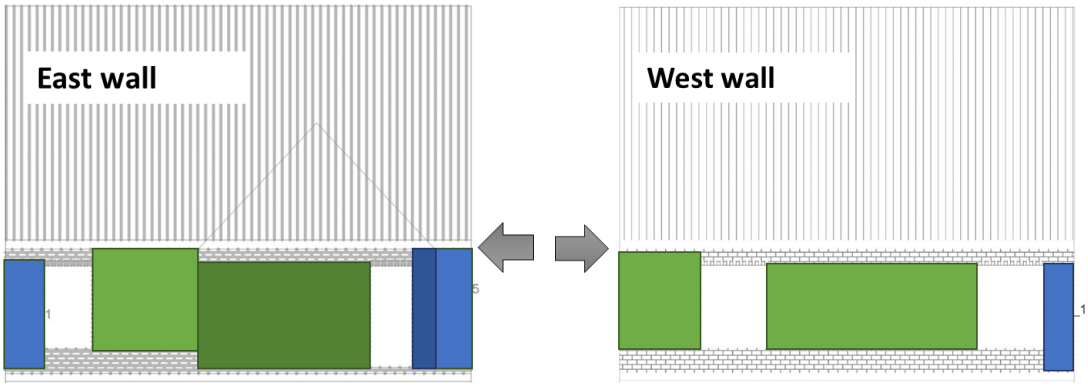

Figure 15. Failure of the piers of the east and west wall for positive loading in the Y-direction. The blue colour represents a flexural failure and the green colour a shear failure.

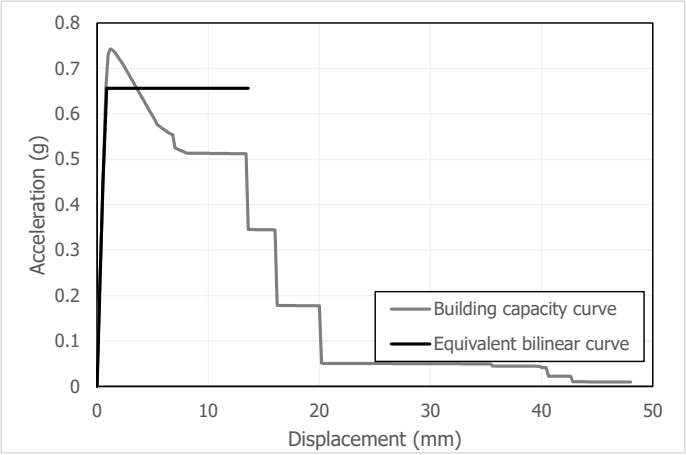

Figure 16. Equivalent bilinear capacity curve derived for the mode-proportional NLPO.

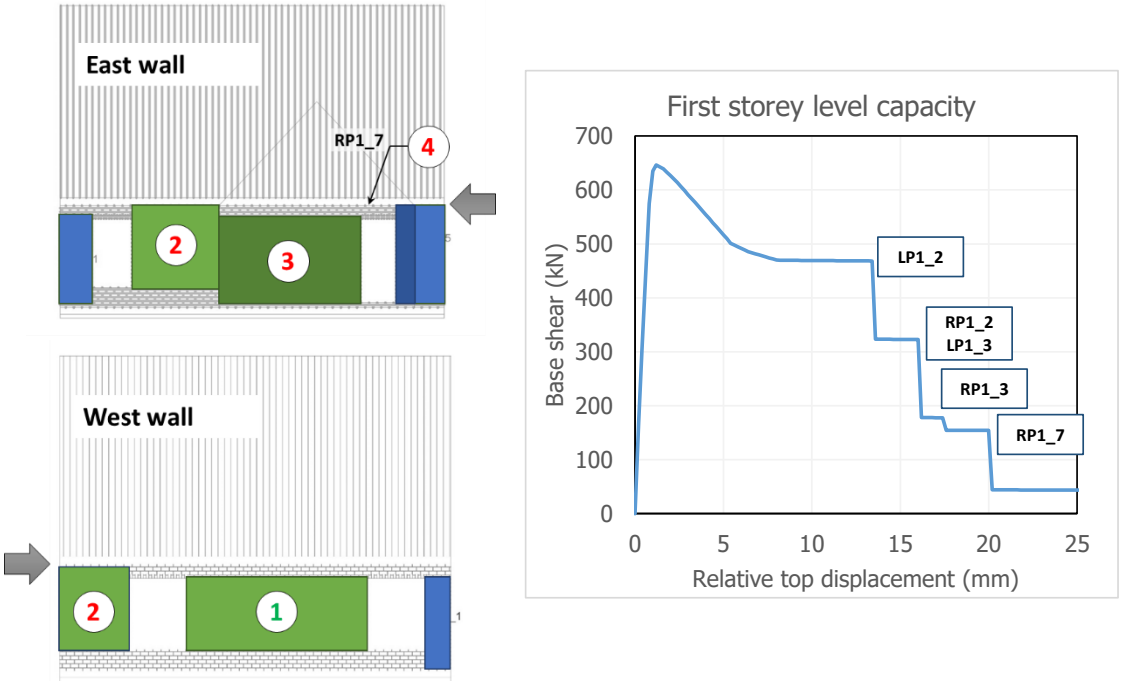

Figure 17. Sequence of NC collapse of the piers on the east and west walls. The piers with a green number fail before the 50% drop, whereas those with a red number fail after that point.

The compliance of the building to NPR9998 is assessed for a specific site by comparing the bilinear capacity curve with the nonlinear ADRS demand. As shown in Figure 18, the building complies to NPR9998 as regards the global in-plane capacity, since the performance point can be find on the capacity curve for a displacement of 0.5 mm, still in the elastic branch of the capacity curve. At this displacement, the system has a ductility factor of 1, so that the elastic ADRS curve is considered.

The spectrum which corresponds to a unity capacity over demand (C/D) ratio is defined by scaling the initial spectrum considered for the site-specific assessment. It should be noted that in principle this is not correct, since each location has several parameters which define the corresponding spectrum and these parameters do not change proportionally. However, the calculation provides a reasonable estimate of the maximum PGA for which the building remains compliant to the NPR9998 recommendations. The scaled spectrum has a PGA of 0.338 g, as shown in Figure 19.

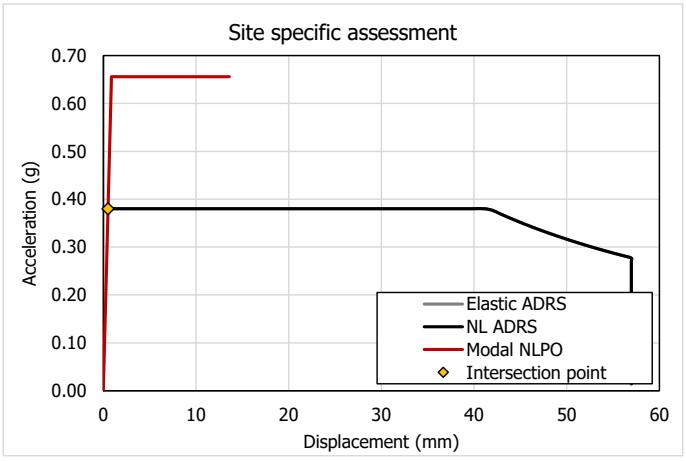

Figure 18. Site specific assessment for mode-proportional NLPO.

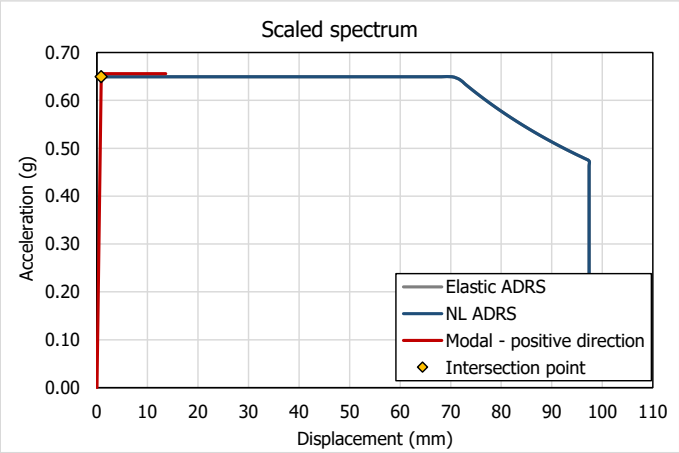

Figure 19. Scaled PGA assessment for mode-proportional NLPO.

3.3 Positive X-direction (West-to-East)

Unlike the Y-direction, in the X-direction the loadbearing piers are located at both the ground storey and the first storey level. The presence of a stiff concrete floor at the first storey allows for the definition of a single capacity curve for the ground storey level; conversely, the piers at the first storey level belong to four lines which are in fact disconnected one to the other (the timber floor is considered as flexible diaphragm). For this reason, three capacity curves are computed: one for the ground floor and two for the first storey level. Two additional wall lines are considered at the first storey level, grouping the non-loadbearing piers. For these walls, the force capacity is normalized with respect to the self-weight of the pier. The wall lines at the first storey level are shown in Figure 20.

The capacity curve obtained for the ground storey level and for the wall lines at the first storey are shown in Figure 21. The minimum capacity in terms of accelerations is found for the ground floor. However, the capacity of the piers of the first storey on the North wall is almost the same, so that the failure of those piers cannot be excluded. However, such piers have a larger ductility, so that overall they should be less vulnerable. A global mechanism at the ground floor level is therefore predicted. The capacity of the internal non-loadbearing walls is significantly larger than that of the ground floor, so that their failure is not expected.

The mode-proportional distribution of the lateral loads is once more governing.

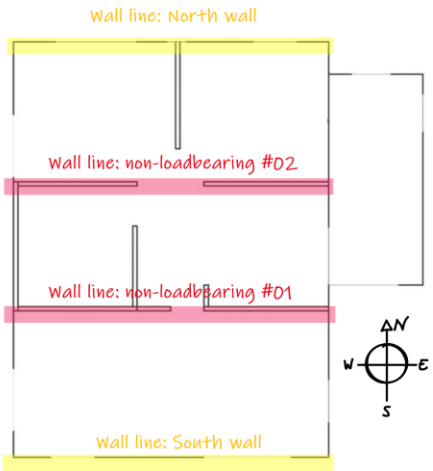

Figure 20. Wall lines defined at first storey level (yellow for the two loadbearing facades and red for the internal non-loadbearing walls)

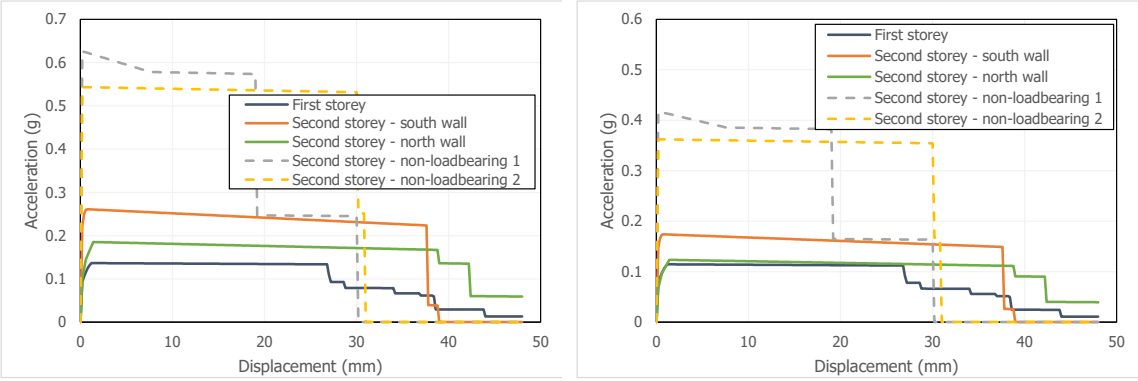

Figure 21. Capacity curve of the ground (a) and first (b) storey level for the positive loading direction.

The type of failure observed in each pier (either shear – as described in section G.9.2.2 of NPR9998 – or flexure – section G.9.2.3) is shown in Figure 22. The blue colour represents flexural failure and the green colour shear failure. All the piers, including the internal non-loadbearing piers except one on the wall line #01, undergo ductile flexural failure.

The "ductile" behaviour is shown also by the equivalent bilinear curve derived for the structure and shown in Figure 23 (for the governing mode-proportional lateral load distribution). This curve shows a yielding point at 0.29 mm, for an acceleration of 0.113g, and a NC displacement at 34.0 mm, corresponding to a 1.25% interstorey drift, consistent with the limitations recommended at global level.

The near collapse (NC) displacement is computed at the point corresponding to a 50% drop of the force capacity with respect to the peak load, because the sequence of failure of the piers (shown in Figure 24) shows that the piers fail in different locations of the building: South wall, then two internal piers and on the North wall before the NC displacement is achieved. In Figure 24 the piers with a green number fail before the 50% drop, whereas those with a red number fail after that point.

The compliance of the building to NPR9998 is assessed for a specific site by comparing the bilinear capacity curve with the nonlinear ADRS demand. As shown in Figure 25, the building complies to NPR9998 as regards the global in-plane capacity, since the performance point can be find on the capacity curve for a displacement of 32.1 mm. At this displacement, the system has an extremely large ductility factor (110), so that the non-elastic ADRS curve is scaled by a factor $\eta = 0.56$.

The spectrum which corresponds to a unity capacity over demand (C/D) ratio is defined by scaling the initial spectrum considered for the site-specific assessment. It should be noted that in principle this is not correct, since each location has several parameters which define the corresponding spectrum and these parameters do not change proportionally. However, the calculation provides a reasonable estimate of the maximum PGA for which the building remains compliant to the NPR9998 recommendations. The scaled spectrum has a PGA of 0.209 g, as shown in Figure 26.

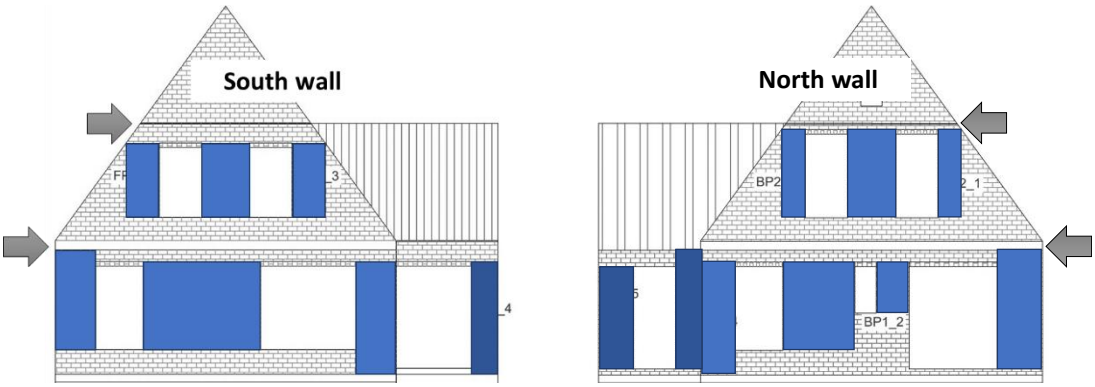

Figure 22. Failure of the piers of the east and west wall for positive loading in the X-direction. The blue colour represents a flexural failure and the green colour a shear failure.

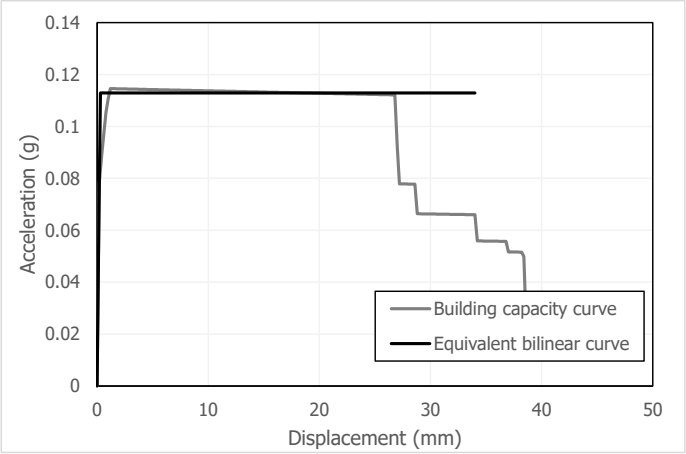

Figure 23. Equivalent bilinear capacity curve derived for the mode-proportional NLPO.

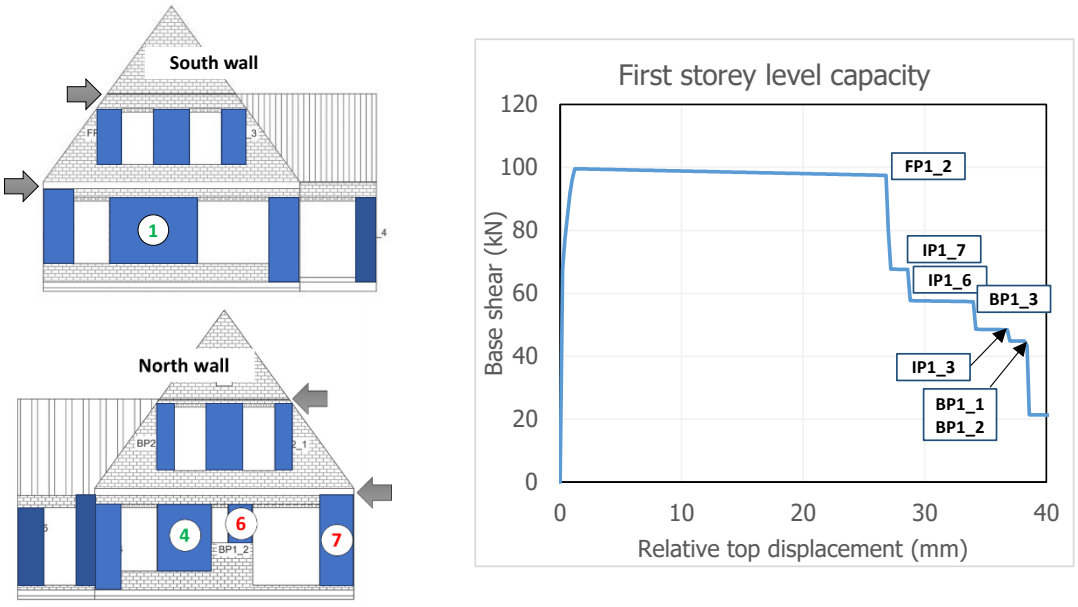

Figure 24. Sequence of NC collapse of the piers on the south and north walls. The piers with a green number fail before the 50% drop, whereas those with a red number fail after that point.

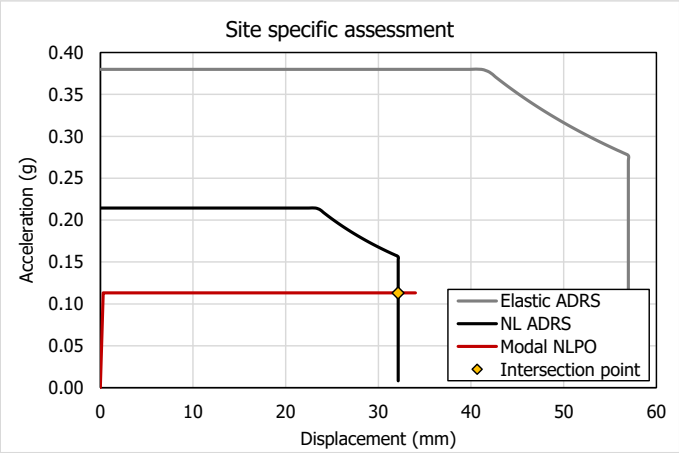

Figure 25. Site specific assessment for mode-proportional NLPO.

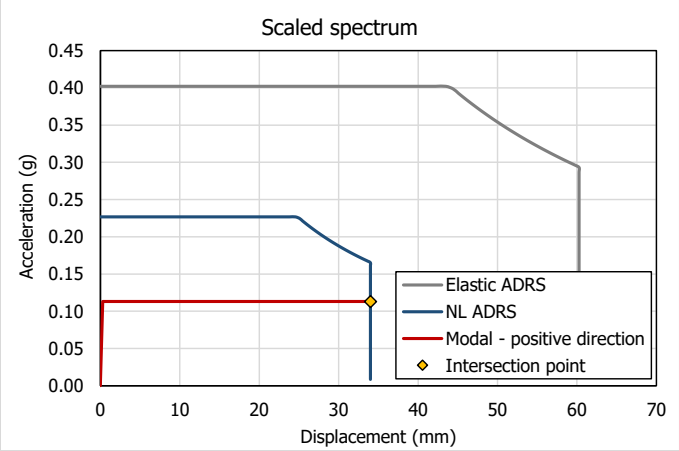

Figure 26. Scaled PGA assessment for mode-proportional NLPO.

3.4 Negative X-direction (East-to-West)

Similar to the positive loading direction, also in the negative X-direction three capacity curves are computed: one for the ground floor and two for the first storey level (and, additionally, two wall lines for the non-loadbearing piers), as shown in Figure 20.

The capacity curve obtained for the ground storey level and for the wall lines at the first storey are shown in Figure 27.

The minimum capacity in terms of accelerations is found for the ground floor. A global mechanism at the ground floor level is therefore predicted. The capacity of the internal non-loadbearing walls is significantly larger than that of the ground floor, so that their failure is not expected.

The mode-proportional distribution of the lateral loads is governing also for this case.

The type of failure observed in each pier (either shear – as described in section G.9.2.2 of NPR9998 – or flexure – section G.9.2.3) is shown in Figure 22. The blue colour represents flexural failure and the green colour shear failure. All the piers, including the internal non-loadbearing piers except one on the wall line #01, undergo ductile flexural failure.

The "ductile" behaviour is shown also by the equivalent bilinear curve derived for the structure and shown in Figure 23 (for the governing mode-proportional lateral load distribution). This curve shows a yielding point at

0.26 mm, for an acceleration of 0.097g, and a NC displacement at 28.6 mm, corresponding to a 1.07% interstorey drift. This value is smaller than the limitations recommended at global level because the global behaviour is largely affected by the collapse of two piers on the north and south walls and of one internal pier, all having small aspect ratio (around 0.7).

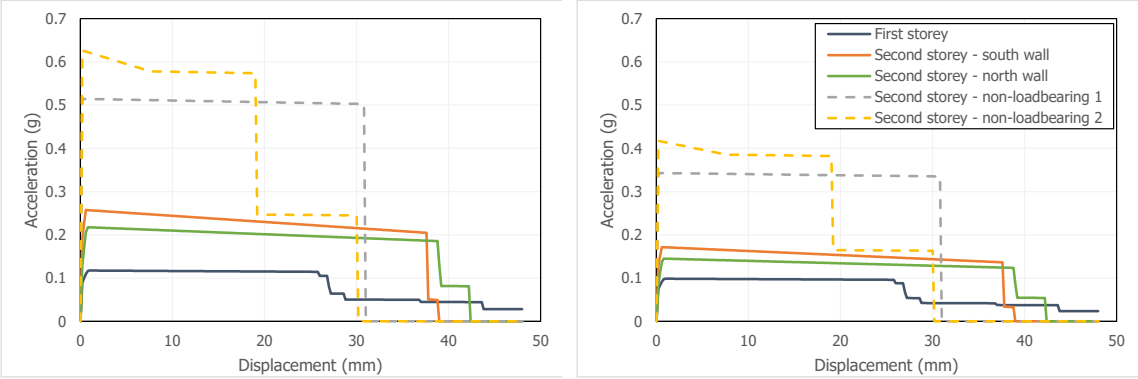

(a) (b)

Figure 27. Capacity curve of the ground (a) and first (b) storey level for the positive loading direction.

The near collapse (NC) displacement is computed at the point corresponding to a 50% drop of the force capacity with respect to the peak load, because the sequence of failure of the piers (shown in Figure 24) shows that the piers fail in different locations of the building: a pier on the South wall, then a pier on the North wall, and finally two internal piers before the NC displacement is achieved. In Figure 24 the piers with a green number fail before the 50% drop, whereas those with a red number fail after that point.

The compliance of the building to NPR9998 is assessed for a specific site by comparing the bilinear capacity curve with the nonlinear ADRS demand. As shown in Figure 31, the building does not comply to NPR9998 as regards the global in-plane capacity, since the performance point cannot be find on the capacity curve. The maximum ductility of the system has been considered, so that the non-elastic ADRS curve is scaled by a factor $\eta = 0.56$.

The spectrum which corresponds to a unity capacity over demand (C/D) ratio is defined by scaling the initial spectrum considered for the site-specific assessment. It should be noted that in principle this is not correct, since each location has several parameters which define the corresponding spectrum and these parameters do not change proportionally. However, the calculation provides a reasonable estimate of the maximum PGA for which the building remains compliant to the NPR9998 recommendations. The scaled spectrum has a PGA of 0.176 g, as shown in Figure 32.

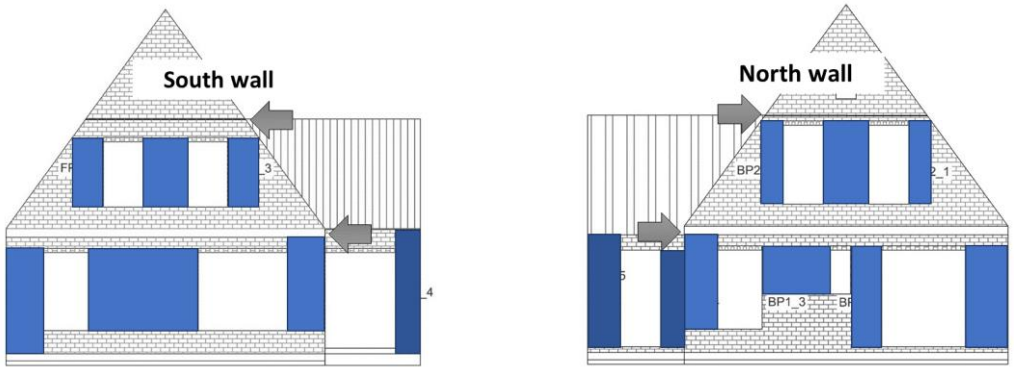

Figure 28. Failure of the piers of the east and west wall for positive loading in the Y-direction. The blue colour represents a flexural failure and the green colour a shear failure.

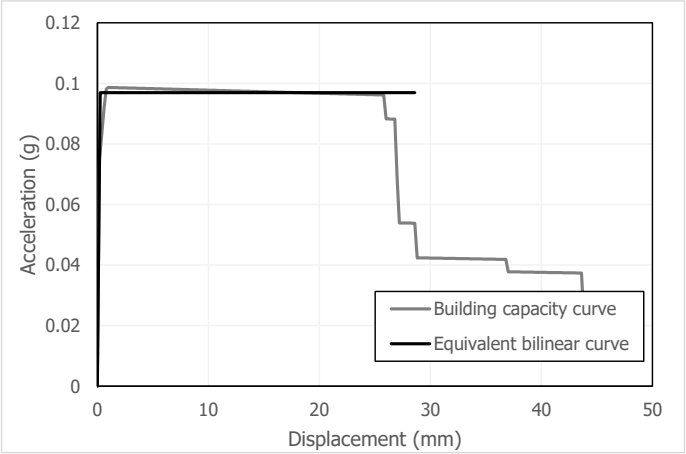

Figure 29. Equivalent bilinear capacity curve derived for the mode-proportional NLPO.

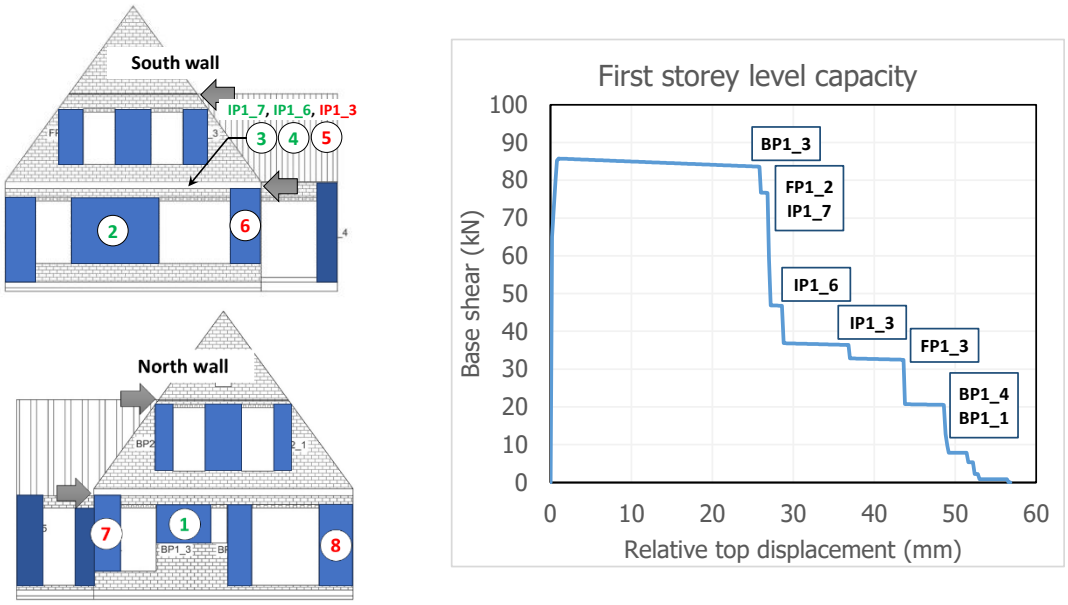

Figure 30. Sequence of NC collapse of the piers on the north and south walls. The piers with a green number fail before the 50% drop, whereas those with a red number fail after that point.

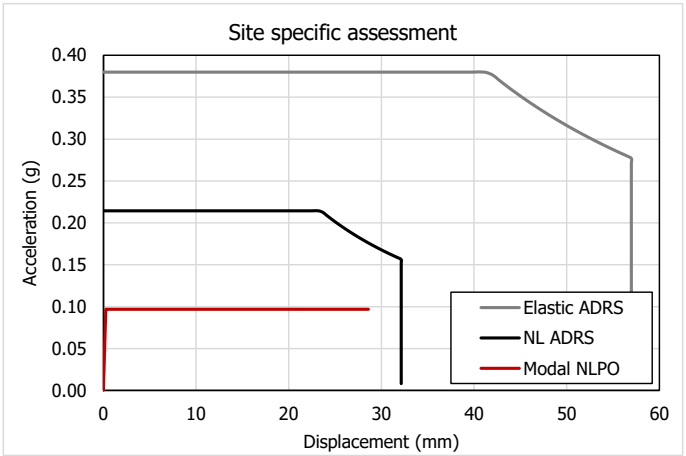

Figure 31. Site specific assessment for mode-proportional NLPO.

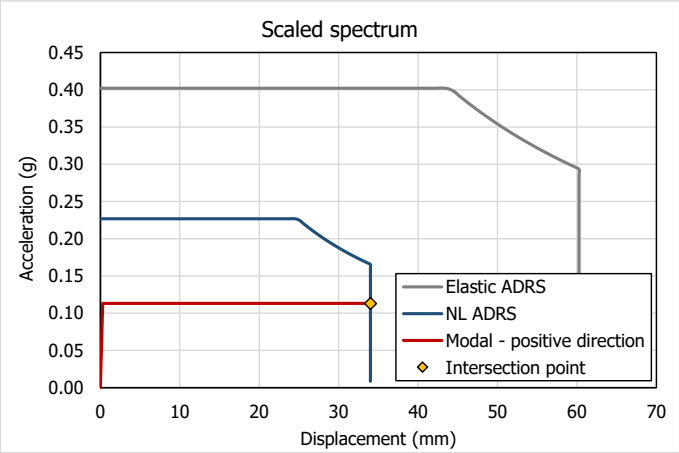

Figure 32. Scaled PGA assessment for mode-proportional NLPO.

4 Summary of the performance of the building

This section summarizes the main results reported for the four cases described in the previous section. Figure 33 shows the bilinear capacity curves computed for the four cases, whereas Table 1 summarizes the most relevant results.

The behaviour of the building is very different in the two loading directions: in the Y-direction the building is characterised by large acceleration capacity and small displacements; conversely, in the X-direction the acceleration capacity is much smaller, although this is partly compensated by larger displacement capacity. This outcome is partially due to the geometry of the building, with long piers at ground floor on the east and west walls, and partially to the spanning direction of the RC slab of the first floor (supported on the east and west walls only). The presence of this floor results, in the initial conditions, in reduced overburdens acting on the piers at the ground storey of the north and south façades (<0.1 MPa, whereas the corresponding values range between 0.3 MPa and 1.5 MPa), which lead to flexural failure and small base shear resistance.

The building does not comply to NPR9998 as regards the global in-plane capacity, due to the assessment for the mode-proportional pushover curve computed in the negative X-direction (east to west). The spectrum which corresponds to a unity capacity over demand (C/D) ratio is defined by scaling the initial spectrum considered for the site-specific assessment and it is estimated with a PGA of 0.176 g.

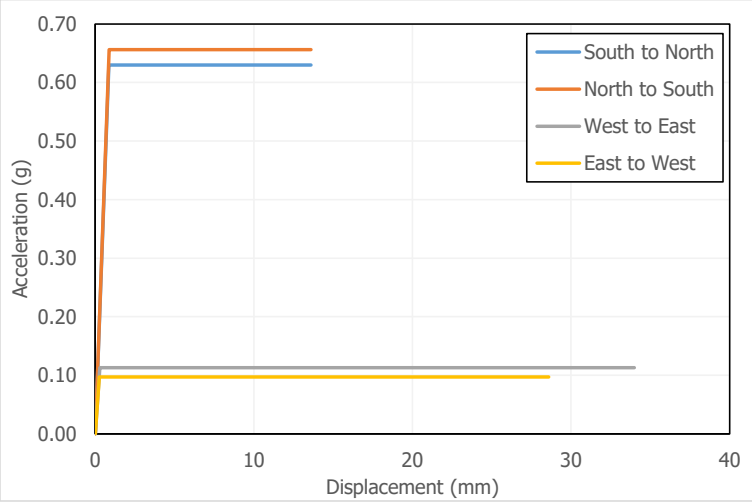

Figure 33. Bilinear capacity curves for the different loading directions

Table 1. Summary of the main results of the SLaMA NLPO for the four loading directions

Direction	Governing storey level	Type of failure	Governing lateral load distribution	a_{max} (g)	d_{NC} (mm)	Site specific C/D	Max PGA (g)
X-positive	Ground storey	Ductile	Mode-proportional	0.11	34.0	1.06	0.209
X-negative	Ground storey	Ductile	Mode-proportional	0.10	28.6	0.89	0.176
Y-positive	Ground storey	Brittle	Mode-proportional	0.63	13.6	1.64	0.325
Y- negative	Ground storey	Brittle	Mode-proportional	0.66	13.6	1.71	0.338

Reference

[1] NEN (2018) - Assessment of the structural safety of buildings in case of erection, reconstruction, and disapproval - Induced earthquakes – Basis of design, actions and resistances. NPR9998:2018, NEN.

[2] NEN (2018) - Webtool NPR 9998: Bepaling van de seismische belasting. Available from URL: http://seismischekrachten.nen.nl/

[3] Yi, T., Moon, F. L., Leon, R. T., & Kahn, L. F. (2008). Flange effects on the nonlinear behaviour of URM piers. The Masonry Society Journal, 26(2), 31-42.